Available online at www.sciencedirect.com
ScienceDirect
Cement and Concrete Research 37 (2007) 1502–1511
Cement and Concrete Research

Correlating cement characteristics with rheology of paste

H. Vikan [a,*], H. Justnes [a], F. Winnefeld [b], R. Figi [b]

[a] SINTEF Building and Infrastructure, Concrete, 7465 Trondheim, Norway
[b] EMPA Swiss Federal Laboratories of Materials Testing and Research, 8600 Dübendorf, Switzerland

Received 28 November 2005; accepted 16 August 2007

Abstract

The influence of cement characteristics such as cement fineness and clinker composition on the "flow resistance" measured as the area under the shear stress–shear rate flow curve has been investigated. Three different types of plasticizers namely naphthalene sulphonate-formaldehyde condensate, polyether grafted polyacrylate, and lignosulphonate have been tested in this context on 6 different cements. The flow resistance correlated well with the cement characteristic (Blaine·{d·cC_3A+[1−d]·C_3S}) where the factor d represents relative reactivity of cubic C_3A and C_3S while cC_3A and C_3S represent the content of these minerals. It was found to be either a linear or exponential function of the combined cement characteristic depending on plasticizer type and dosage. The correlation was valid for a mix of pure cement and cement with fly ash, limestone filler (4%), as well as pastes with constant silica fume dosage, when the mineral contents were determined by Rietveld analysis of X-ray diffractograms.

Keywords: Cement; Flow; Mineralogy; Paste; Rheology

1. Introduction

Some important factors affecting cement paste rheology are summarized as follows [1–4]:

- Water–solid ratio
- Chemical composition of cement
- Chemical reactivity of filler
- Particle size distribution, specific gravity, surface texture and geometrical shape of powders (cement and fillers)
- Properties of chemical admixtures
- Hydration time
- Temperature and humidity of the place where the paste is prepared and placed
- Initial mixing conditions, such as mixing procedure, mixer speed, duration and capacity
- Testing procedure such as test duration, measuring elements, extent of agitation during the period of hydration, geometry of the test accessory, the gap and friction capacity of its shearing surfaces

It has been shown that the most important of the factors listed above are the w/c ratio and the specific surface. Studies performed on cement pastes of different chemical composition indicated this factor bears a less effect on the rheology than w/c ratio and/or fineness of cement [2,5]. Type of plasticizer will, however, also influence the flow properties of cementitious pastes due to their dependencies on cement chemistry, different dispersing mechanisms and retarding effects on the cement paste [6–11].

Finding a rheological model describing the shear stress (τ)–shear rate ($\dot{\gamma}$) flow curve for cementitious pastes has proved to be a challenge. Among the numerous models proposed are:

$$\text{Power–law model: } \tau = K \cdot \dot{\gamma}^n \tag{1}$$

$$\text{Bingham plastic } \tau = \tau_y + \mu_p \cdot \dot{\gamma} \tag{2}$$

$$\text{Herschel–Bulkley } \tau = \tau_y + K \cdot \dot{\gamma}^n \tag{3}$$

$$\text{Robertson Stiff } \tau = A \cdot (\dot{\gamma} + B)^n \tag{4}$$

$$\text{Casson } \tau^{1/2} = \tau_y^{1/2} + \left(\mu_p \cdot \dot{\gamma}\right)^{1/2} \tag{5}$$

* Corresponding author. Tel.: +47 73594565; fax: +47 73597136.
E-mail address: hedda.vikan@sintef.no (H. Vikan).

0008-8846/$ - see front matter © 2007 Elsevier Ltd. All rights reserved.
doi:10.1016/j.cemconres.2007.08.011

$$\text{Sisko } \tau = \mu_\infty \cdot \dot{\gamma} + K \cdot \dot{\gamma}^n \quad (6)$$

$$\text{Eyring } \tau = A \cdot \sinh^{-1} \cdot (B \cdot \dot{\gamma}) \quad (7)$$

$$\text{DeKee } \tau = \tau_y + \mu_p \cdot \dot{\gamma} \cdot \overline{e}^{\alpha \dot{\gamma}} \quad (8)$$

$$\text{VomBerg } \tau = \tau_y + B \cdot \sinh^{-1}\left(\frac{\dot{\gamma}}{C}\right) \quad (9)$$

where A, B and C are constants, τ_y is a yield stress parameter, μ_p is a plastic viscosity, α is a time dependent parameter, K is the "consistency" [Pa·s^n] and n is the power law index. The Robertson–Stiff model becomes equal to the Bingham model if n is equal to 1, giving τ_y equal to AB and the plastic viscosity as A. The model becomes equivalent to the Newton model when B is equal to 0 and n is equal to 1. Herschel–Bulkley also becomes equal to Bingham when $n=1$.

Turian et al. [12] investigated the rheology of concentrated aqueous slurries of titanium dioxide, laterite, gypsum and silica flour. The two-parameter power law, Bingham plastic and Casson models and the three-parameter Herschel–Bulkley and Sisko models were tested. The Sisko model which combines low- and intermediate shear power law with high shear Newtonian limiting behaviour, was found to provide the best overall description of the flow curves for all slurries, at all solid loadings and over the entire range of shear rates.

Yahia and Khayat [13] evaluated the effectiveness of various rheological models to estimate yield stress of high-performance cement grouts containing supplementary cementitious materials and rheology-modifying admixtures. The rheological models considered in the investigation included Bingham, Casson, Herschel–Bulkley and De Kee as well as a model proposed by the authors. Different estimates of the yield value were obtained when using the different models. The Bingham model resulted in higher yield stress estimates than the other models, while the Herschel–Bulkley model resulted in the lowest values for all tested mixtures.

Atzeni et al. [14] found from their investigations that the best results for fitting the rheological data of Portland cement pastes were obtained with Eyring's, Herschel–Bulkley and the parabolic equation, while Vom Berg's model only held for low shears. The authors proposed another equation derived from Eyring's, but explicitly containing the yield stress term.

Yahia and Khayat [15] investigated the Bingham, Herschel–Bulkley, Casson, Eyring, Robertson–Stiff, De Kee and Vom Berg model on high-performance grouts containing supplementary cementitious materials and viscosity enhancing admixture. They found that none of the evaluated models could enable accurate fitting of shear stress–shear rate data of all investigated mixtures. Difficulties were mostly encountered modeling the non-linear portion of the flow curve observed at the low shear rate range.

Rheological measurements done for this paper indicated that the cement pastes often showed shear thinning or shear thickening behaviour. The results illustrated moreover that models such as Bingham and Herschel–Bulkley did not describe the flow of cementitious pastes satisfactorily. It was for instance difficult to compare the consistencies (K) derived from the Herschel–Bulkley model due to its dimension [Pa·s^n] which is depending on n. Plastic viscosities for different mixes with different n-factors and sometimes the yield stress, τ_y, became negative with no physical meaning. Also linear flow curves, in particular in the medium rate range for mixes showing some shear thickening, lead to negative yield stress. For instance this data set; plastic viscosity 157 mPa·s and yield stress −5.6 Pa (negative) with a regression factor of $R^2=0.9982$. Thus, it was decided to use the area under the flow curve as an alternative rheological parameter to correlate with the cement characteristics. This parameter will always be a positive value and not depend on the curve shape. Furthermore, the choice between two parameters for correlation, as for the Bingham model, can be omitted. Gad et al. [16] has found in a similar study that the area under the shear rate curve is an energy parameter which they considered as a quantitative expression linked to flow properties of cementitious pastes. The area is obtained by multiplying the average yield stress, τ, with average shear rate, γ, in each shear rate step, and it will have the unit Pa/s.

In a parallel plate set-up with shear area, A [m^2], and gap h [m] between the plates;

$$\tau = F/A\left[\text{N/m}^2 \text{or Pa}\right] \quad (10)$$

$$\dot{\gamma} = v/h\left[\text{m/s} \cdot \text{mors}^{-1}\right] \quad (11)$$

where F [N] is the force used to rotate the upper plate and v [m/s] is the velocity.

$$\text{Area under the curve} = \tau \cdot \dot{\gamma} = (F/A) \cdot (v/h) = F \cdot v/A \cdot h = F \cdot v/V$$

where V [m^3] is the volume of the sample. The unit of the area under the curve is then [N·m/m^3·s or J/m^3·s or W/m^3]. It is in other words the power required to make a unit volume of the paste flow with the prescribed rate in the selected range. The power, P [W], required to mix concrete for a certain time interval is actually sometimes measured by simply monitoring voltage (U [V]) and current (I [A]) driving the electrical motor of the mixer, since $P=U \cdot I$. The area under the curve was called "flow resistance" since it represents the required power to move a unit volume of paste. The flow resistance could have been obtained at constant shear rate, but a shear rate range was used in order to compare with parameters from the Bingham model. An alternative is also to use the torque of the rheometer directly.

2. Materials used

2.1. Cementitious materials

Six different Portland cements were tested (5 Norwegian and 1 Swiss) with chemical analyses as listed in Table 1, physical characteristics as shown in Table 2 and mineralogy obtained by quantitative X-ray diffraction (QXRD) and Rietveld analyses as reproduced in Table 3. The Rietveld method is a tool which is proven to be more accurate for a quantitative analysis of clinker and anhydrous cementitious materials than the Bogue calculation

and can be compared with the phase quantification obtained by optical microscopy (point counting) [17,18]. The absolute errors of quantification of the Portland cement by the Rietveld method in this study have been estimated by comparing the results from earlier performed analysis with alternative methods like microscopy or thermoanalysis to be as follows:

- Values lower than 0.5% are doubtful since they are within the uncertainty range of the method.
- Values below 3% has an error of +/−0.4%
- Values within 10–20% has an error of +/−1%
- Values >30% has an error of +/−2%
- Determination of amorphous phases <20% has an error of +/−4%
- Determination of amorphous phases >20% has an error of +/−2%

In order to study the effect of cement fineness on the flow resistance of paste, one clinker was ground with a constant amount of sufficient gypsum to control set to different finenesses covering the range for commercial cements. The mineral composition of the cements can be found in Table 4.

Silica fume (SF) was obtained from the ferro-silicon manufacturer Elkem, Norway, and consisted of 94.7% SiO_2 with a specific surface of 22 m^2/g (N_2 adsorption, BET).

Table 1
Chemical analysis (%) of the Portland cements according to producer and minerals (%) by Bogue estimation

Cement no.	1	2	3	4	5	6
Cement type	CEM I 42.5 RR	CEM I 42.5 R	CEM II A-V 42.5 R	CEM I 52.5 R-LA	CEM I 42.5 R-LA	CEM I 42.5 N
Chemical analyses						
CaO	61.98	62.25	–	63.71	63.15	63.3
SiO_2	20.15	19.69	–	20.92	21.98	19.7
Al_2O_3	4.99	4.55	–	4.21	3.47	5.3
Fe_2O_3	3.36	3.41	–	3.49	5.13	2.7
SO_3	3.55	3.43	2.68	2.67	2.26	2.7
MgO	2.36	2.32	–	1.87	1.56	1.9
Free CaO	1.23	0.87	0.78	0.84	0.94	–
K_2O	1.08	1.15	–	0.46	0.54	0.87
Na_2O	0.42	0.41	–	0.19	0.21	0.33
Equiv. Na_2O	1.13	1.17	–	0.49	0.57	0.90
Cr^{6+} (ppm)	0.00	5.30	5.00	0.30	–	–
Carbon	0.04	0.55	–	0.17	–	–
Chloride	0.03	–	–	0.02	–	0.03
LOI	1.34	2.93	1.82	1.72	0.90	–
Fly ash	–	–	16.3	–	–	–
Minerals by Bogue[a]						
C_3S	50.7	48.1	–	50.4	53.0	51.0
C_2S	19.5	20.2	–	22.0	23.0	18.0
C_3A	7.5	6.3	–	5.3	0.5	9.5
C_4AF	10.2	10.4	–	10.6	15.6	8.2
$C\bar{S}$	7.7	7.4	–	5.8	4.9	5.8

Cement 3 is produced of 1 part Cement 4, 3 parts Cement 2 and 1 part fly ash.
[a] Taking into account SO_3 and $CaCO_3$ from QXRD (Table 3).

Table 2
Physical characteristics of Portland cements according to EN 196

Cement no.	1	2	3	4	5	6
Cement type	CEM I 42.5 RR	CEM I 42.5 R	CEM II A-V 42.5 R	CEM I 52.5 R-LA	CEM I 42.5 R-LA	CEM I 42.5 N
Fineness:						
Grains +90 μm	0.1%	2.9%	0.0%	1.7%	0.0%	0.0%
Grains +64 μm	0.5%	6.6%	0.2%	4.1%	0.6%	3.8%
Grains −24 μm	89.2%	63.1%	83.0%	66.3%	86.6%	–
Grains −30 μm	94.8%	71.2%	90.3%	75.6%	93.3%	–
Blaine (m^2/kg)	546	360	467	359	450	315
Water demand	32.0%	26.8%	29.4%	26.7%	28.2%	27.2%
Le Chatelier	0 mm	0 mm	0.3 mm	0.5 mm	0.0 mm	1.0 mm
Initial set time	115 min	140 min	125 min	145 min	100 min	171 min
σ_c (MPa) at						
1 day	32.7	19.7	22.5	17.1	21.7	–
2 days	39.9	32.7	32.1	27.5	32.5	26.8
7 days	49.3	43.5	43.8	42.5	46.1	–
28 days	58.9	51.2	57.1	58.6	62.0	59.2

2.2. Plasticizers

Three different classes of plasticizers were tested. The lignosulphonate plasticizer Ultrazine Na was delivered by Borregaard Lignotech, Norway, as a powder and diluted to a

Table 3
Mineral composition (%) of Portland cements obtained by QXRD and content of water soluble alkali determined by Plasma emissions spectrometry

Cement no.	1	2	3	4	5	6
Cement type	CEM I 42.5 RR	CEM I 42.5 R	CEM II A-V 42.5 R	CEM I 52.5 R-LA	CEM I 42.5 R-LA	CEM I 42.5 N
Alite	64.7	66.0	60.3	65.0	61.9	51.6
Belite	14.8	9.4	7.1	12.9	19.7	17.3
Ferrite	7.5	8.7	7.1	9.6	12.0	5.4
Cubic aluminate	5.9	3.4	3.1	0.5	0.4	3.6
Orthorhombic aluminate	1.1	1.7	3.4	3.0	1.7	8.7
Lime	1.0	1.2	0.2	0.6	0.7	0.4
Periclase	1.6	1.2	1.7	0.3	0.4	0.9
Gypsum	0.0	0.2	0.0	1.4	1.3	3.2
Hemihydrate	1.8	2.0	2.1	1.5	0.4	1.2
Anhydrite	0.6	0.5	0.4	0.4	0.4	0.8
Calcite	0.5	4.6	0.6	4.0	0.7	4.3
Portlandite	0.3	0.4	0.5	0.3	0.2	0.4
Quartz	0.0	0.4	1.5	0.4	0.2	0.4
Arcanite	0.3	0.4	0.1	0.0	0.0	1.8
Mullite	–	–	2.6	–	–	–
Amorphous	–	–	9.3	–	–	–
K (%)	0.92	0.88	0.58	0.32	0.36	0.42
Na (%)	0.22	0.17	0.12	0.07	0.08	0.04
Na_{eqv} (%)	0.76	0.69	0.46	0.26	0.30	0.29

Table 4
Characteristics of 4 cements made of the same clinker, but ground to different fineness (Blaine)

Blaine	SO_3	Free lime	Loss of ignition	SiO_2	Al_2O_3	Fe_2O_3	CaO	K_2O	MgO	Na_2O	Alkali
496	2.97	0.90	1.11	20.47	4.83	3.34	62.48	1.06	2.29	0.45	1.15
444	2.92	0.90	1.06	20.50	4.87	3.33	62.47	1.07	2.30	0.44	1.14
392	2.94	0.81	1.15	20.47	4.77	3.34	62.44	1.06	2.26	0.45	1.15
356	3.00	0.69	1.17	20.10	4.60	3.28	62.48	1.05	2.21	0.41	1.10

30% solution prior to use. The superplasticizer sodium naphthalene sulphonate-formaldehyde condensate (abbreviated SNF) was of the type Mighty 150 produced by Kao, Japan, a solution with 42% solids. The superplasticizer RN-15 was a product of Rescon-Mapei, Norway, with 20% active polymer as a polyacrylate backbone with grafted polyether side chains.

3. Experimental

3.1. Rheology

Cement pastes (150 ml) were made with a constant total particle volume fraction of 0.442, corresponding to about w/c=0.40 as basis, using distilled water, and with SF replacing cement by volume fraction 0.00 or 0.03 (corresponding to mass SF of total powder of 0.0 or 4.8%, alternatively 0.0 or 6.8vol.%). The blending was performed in a high shear mixer from Braun by adding solids to the water and mix for 1/2 min, resting for 5 min and blending again for 1 min. 0.53% by cement weight of SNF, lignosulphonate or polyacrylate was added to the pastes. The admixtures were added in the water first (momentary addition).

The rheological parameters were recorded by a parallel plate (1 mm gap, upper plate serrated to 150 μm depth) rheometer MCR 300 from Physica. The following sequence lasted 25 min; it was started when the paste was 20 min old after water addition and repeated 4 times to monitor time dependencies:

- Shear stress (τ)–shear rate ($\dot{\gamma}$) curve with linear sweep of $\dot{\gamma}$ from 200 down to 2 s^{-1} in 30 points lasting 6 s each (intervals 1, 7, 13 and 19 lasting 3 min).
- Shear stress (τ)–shear rate ($\dot{\gamma}$) curve with linear sweep of $\dot{\gamma}$ from 2 up to 200 s^{-1} in 30 points lasting 6 s each (intervals 2, 8, 14 and 20 lasting 3 min).
- 10 s resting as 5 points lasting 2 s each had no recording (intervals 3, 9, 15 and 21)
- Shear rate ($\dot{\gamma}$)–shear stress (τ) curve with logarithmic sweep of τ from 0.2 to 50 Pa in 46 points lasting 5 s each (intervals 4, 10, 16 and 22 lasting 3 min and 50 s each) to measure gel strength after 10 s rest.
- Oscillatory time sweep with 30 points lasting 20 s each with amplitude γ=0.1% and angular frequency ω=6 s^{-1} (intervals 5, 11, 17 and 23 lasting 10 min) measuring storage and loss moduli G′ and G″.
- Shear rate ($\dot{\gamma}$)–stress (τ) curve with logarithmic sweep of τ from 0.5 to 200 Pa (range may vary) in 60 points lasting 5 s each (intervals 6, 12, 18 and 24 lasting 5 min each) to measure gel strength after 10 min rest (i.e. oscillation).

Only the shear stress–shear rate down curve has been used in the following correlations. The whole measurement sequence has been listed here to illustrate the shear history of the pastes.

Full rheological measurement sequence was also performed on cement pastes with plasticizers added in dosages of 0–2% by weight to study the effect of plasticizer type and dosage.

3.2. Setting times

An 8 channel TAM Air Isothermal Calorimeter from Thermometric AB, Sweden was used for measuring the heat

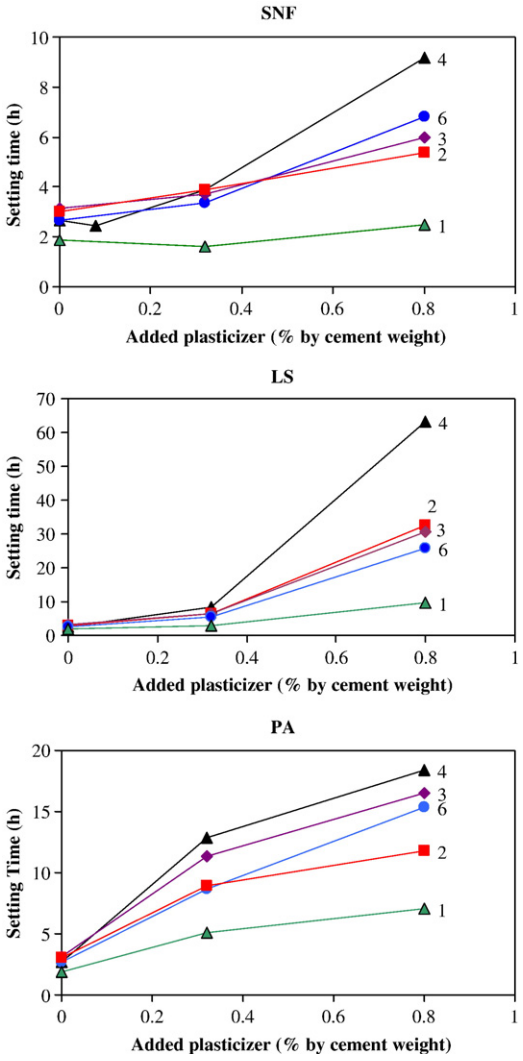

Fig. 1. Setting times of cements 1–4 and 6 as a function of SNF, lignosulphonate (LS) and polyacrylate (PA) dosage.

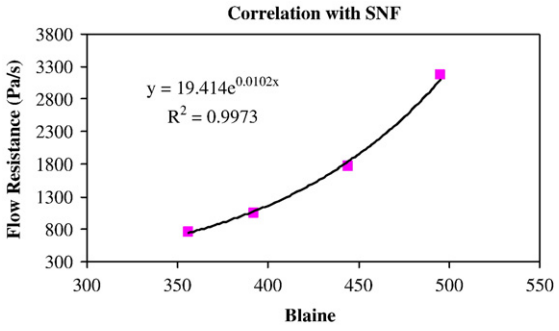

Fig. 2. Correlating flow resistance in the medium shear rate range with surface area of cements originating from the same clinker, but ground to different finenesses (see Table 4).

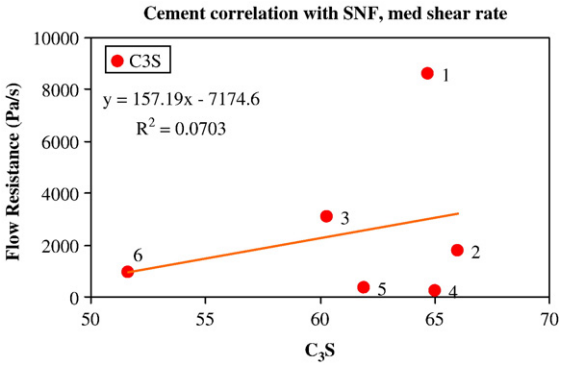

Fig. 4. Correlating the amount of C_3S for 6 cements with area under the medium shear rate range of the flow curve for respective pastes with w/c ≈ 0.40. 1st run (20 min from water addition) of pastes with 0.53% SNF.

of hydration for the various cement-plasticizer combinations. The calorimeter was calibrated at 20 °C whereby the baselines of the calorimeter were determined. 6 g of cement was weighed into glass ampoules. 2.40 g of liquid was added to each sample (corresponding to w/c = 0.4). The dosage of superplasticizer was 0.0, 0.32% and 0.80% of cement weight for the three plasticizers lignosulphonate, polyacrylate and SNF. The samples were mixed in a motorized stirrer (IKA-WERK, RM 18 (60 Watt)) from Janke & Kunkel KG, for 2 min and the exact weight of the cements were noted. The ampoule was sealed with an aluminium cap and wiped with a paper napkin to make sure that it was perfectly clean and dry when it was inserted into the calorimeter. The heat of hydration measurement was logged until 72 h after water addition. The initial setting times for the different cement-plasticizer combinations were determined from the calorimetric curves at the end of the dormant period.

3.3. Plasticizer saturation dosage

A UV Spectrophotometer from Thermo Spectronic was used to measure the adsorbed amounts of SNF and lignosulphonate on the cement. The superplasticizer saturation dosage was defined at the point where any further addition of superplasticizers does not significantly reduce the flow resistance of the slurry.

The pore solutions were extracted from the cementitious pastes by filtering the pastes through 0.45 μm-filters 20 min after water addition. They were then diluted 100–200 times with a solution of "artificial pore water" (NaOH and KOH with a K/Na molar ratio equal to 2 and pH = 13.2). The amount of superplasticizer in the water phase was read from the standard curve which had been made with a dilution series of SNF (290 nm) and lignosulphonate (283 nm). The difference between the added and measured content of superplasticizer gave the bound portion.

Polyacrylate-type products generally do not contain aromatic groups and do not show UV-adsorption in a readily accessible spectral region, i.e. >200 nm (Spiratos et al., 2003). The adsorption of polyacrylate on cement was done by measuring the Total Organic Carbon (TOC) left in the pore water with a Shimadzu TOC Analyzer 5000A. Preparation of pastes and measurement of rheology was done as described above. The pore water was filtrated from the pastes as described above, but diluted 1:10 with 0.1 M HCl. The amount of plasticizer bound to the cement was calculated by difference between the added and the measured content of organic carbon.

4. Results and discussion

4.1. Influence of plasticizer and cement type on the plasticizer saturation dosage

The TOC measurements showed that the cements consumed (i.e. adsorbed and intercalated) less polyacrylate than SNF and

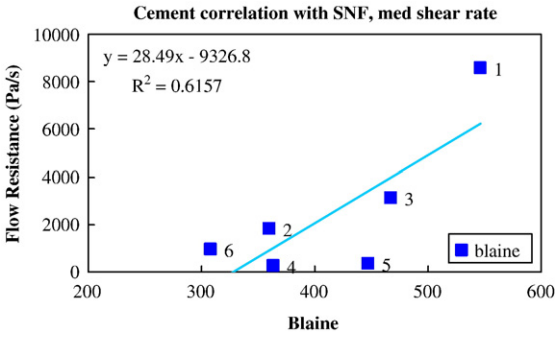

Fig. 3. Correlating the Blaine value of 6 cements with area under the low rate range of the flow curve for respective pastes with w/c ≈ 0.40. 1st run (20 min from water addition) of pastes with 0.53% SNF.

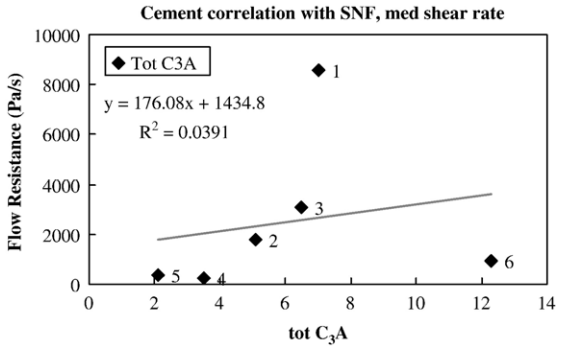

Fig. 5. Correlating the total amount of C_3A for 6 cements with area under the medium shear rate range of the flow curve for respective pastes with w/c ≈ 0.40. 1st run (20 min from water addition) of pastes with 0.53% SNF.

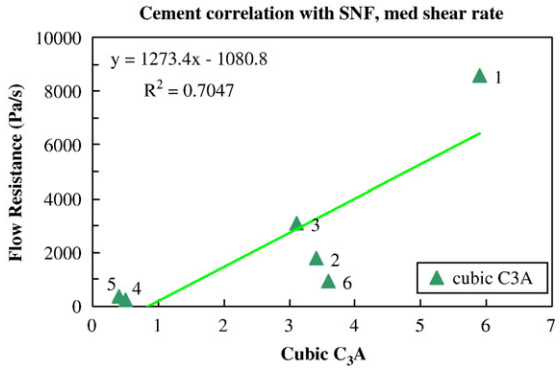

Fig. 6. Correlating the amount of cubic C_3A in 6 cements with area under the medium shear rate range of the flow curve for respective pastes with w/c ≈ 0.40. 1st run (20 min from water addition) of pastes with 0.53% SNF.

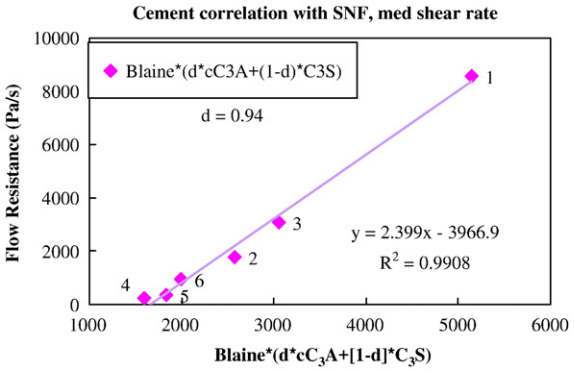

Fig. 8. Correlating the Blaine value multiplied with a weighed sum of cubic C_3A and C_3S for 6 cements with area under the medium shear rate range of the flow curve for respective pastes with w/c ≈ 0.40. 4th run (20 min from water addition) of pastes with 0.53% SNF.

lignosulphonate. Polyacrylate was however found to be the most efficient dispersant of the three plasticizers. Cement 1 required for example 1.20% SNF or 0.32% PA to obtain a flow resistance of approximately 600 Pa/s. This observation is supported by Golaszewski and Szwabowski [19] who found that it was necessary to use approximately twice the dosage of SNF superplasticizer compared to a PA superplasticizer (especially for low w/c mortars) to obtain a specific value of yield stress by the Bingham model. On the other hand, viscosity values of mortars made with PA superplasticizer was up to three times higher than for that of mortars with SNF superplasticizer. Hanehara and Yamada [20] found that the slump area ratio (paste spread) of a cement paste prepared by adding as little as 0.2% of polycarboxylic acid-based admixture increased enough to improve fluidity. Meanwhile, the fluidity of cement paste prepared using naphthalene sulphonic acid-based admixture was hardly changed by adding up to 0.8% of the admixture.

4.2. Influence of plasticizer type on setting time

The retardation of the setting time will depend on the cement as well as the plasticizer type. For instance, a low content of C_3A (and low surface area) will result in low consumption of plasticizer. Most of the plasticizer will in this case remain in the solution causing an enhanced retarding effect. Fig. 1 indicates that the setting times are longer for the cements with low content of cubic C_3A and low surface. The figure illustrates moreover that lignosulphonate is the strongest retarder of the three plasticizers at a concentration of 0.80% by cement weight, while polyacrylate is the strongest retarder at a plasticizer dosage of 0.32%. SNF has the least retarding effect on the hydration at both dosages. Further information about the influence of the plasticizer and the cement type on setting time and hydration can be found elsewhere [21].

4.3. Correlating rheology parameters of paste with cement mineralogy

Fig. 2 shows the flow resistance as a function of cement fineness for the four cements originating from the same clinker described in Table 4. The figure illustrates that the flow resistance is an exponential function of the cement fineness (Blaine). Fig. 3 illustrates, however, that cement fineness correlates poorly with flow resistance when the cements originate from different clinkers. This finding illustrates that cement cannot be treated as a univariable material. The flow resistance depends on several factors such as fineness, content of C_3A, alkali etc. and all these factors might increase or decrease from cement to cement pulling the flow resistance

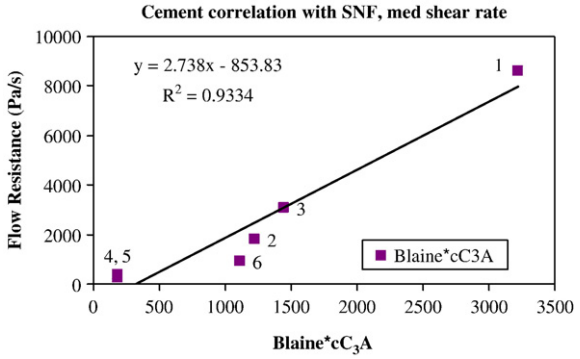

Fig. 7. Correlating the Blaine value multiplied with cubic C_3A for 6 cements with area under the medium shear rate range of the flow curve for respective pastes with w/c ≈ 0.40. 1st run (20 min from water addition) of pastes with 0.53% SNF.

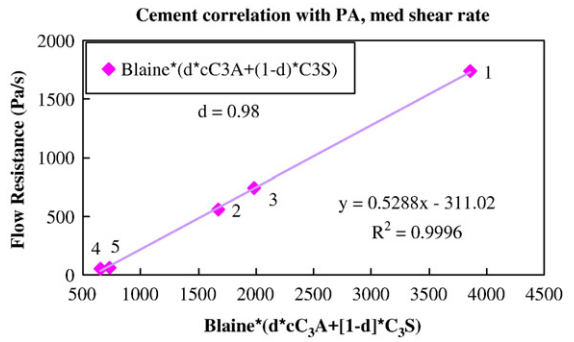

Fig. 9. Correlating the Blaine value multiplied with a weighed sum of cubic C_3A and C_3S for cements 1–5 with area under the medium shear rate range of the flow curve for respective pastes with w/c ≈ 0.40. 1st run (20 min from water addition) of pastes with 0.53% RN-15.

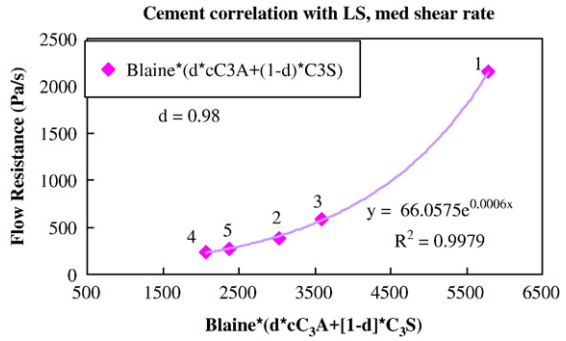

Fig. 10. Correlating the Blaine value multiplied with a weighed sum of cubic C_3A and C_3S for cements 1–5 with area under the medium rate range of the flow curve for respective pastes with w/c ≈ 0.40. 1st run (20 min from water addition) of pastes with 0.53% Ultrazine Na.

values in different directions. Thus, correlations cannot be made between flow and single cement characteristics unless there is only one variable differentiating the cements from each other. This finding is further emphasized by Figs. 4–6 which show attempts of linear correlations with content of C_3S, total C_3A and cubic C_3A respectively. A more promising correlation was however found between flow resistance and Blaine multiplied with cubic C_3A as illustrated in Fig. 7. It is focused on the cubic crystal modification of C_3A since it is known to be more reactive than the orthorhombic crystal modification [22,23]. Thus, the idea behind multiplying cubic C_3A with Blaine is that this parameter represents the amount of active mineral on the surface (excluding the fraction inside the cement grain). However, C_3S is also quite reactive (although less than cubic C_3A) and it is much more of it (e.g. 60% versus 3%). It was therefore decided to include a weighed sum of the two minerals multiplied with Blaine giving the equation

$$\text{Blaine} \cdot \{d \cdot \text{cC}_3\text{A} + (1-d) \cdot \text{C}_3\text{S}\} \quad (13)$$

where the factor d represents relative reactivity and cC_3A and C_3S represent the content of cubic C_3A and C_3S.

Attempts to make a linear correlation of the cement characteristics from Eq. (13) with measured flow resistance

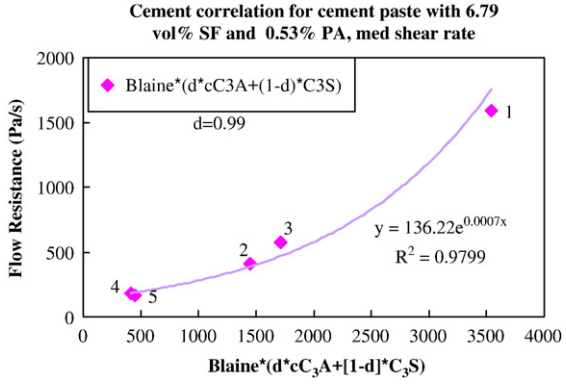

Fig. 11. Correlating the Blaine value multiplied with a weighed sum of cubic C_3A and C_3S for cements 1–5 with area under the medium rate range of the flow curve for respective pastes with 6.97 vol.% silica fume and w/(c+s) ≈ 0.40. 1st run (20 min from water addition) of pastes with 0.53% RN-15.

Table 5
Saturation dosage of SNF and LS for cements 1–5

Cement number and type	Saturation dosage (% by cement weight)	
	SNF	LS
1 CEM I 42.5 RR	1.20	1.20
2 CEM I 42.5 R	0.56	0.80
3 CEM II A-V 42.5 R	0.72	0.64
4 52.5 R-LA	0.32	0.48
5 CEM I 42.5 R-LA	0.56	0.56

for pastes with 0.53% by cement weight of SNF or polyacrylate as plasticizers gave surprisingly good fits (R^2 = 0.9908 and 0.9996 respectively) as depicted in Figs. 8 and 9. The results are surprisingly good since the series contain cements with and without 4% limestone interground as well as one with ≈ 17% Class F fly ash interground. However, using QXRD for the determination of minerals of interest gives the correct value independently of other mineral additions.

The correlation has thus 3 variables (factors a, b and d) and 6 observations (number of cements):

$$\text{Flow Resistance} = a \cdot \text{Blaine} \cdot [d \cdot \{\text{cubic } \text{C}_3\text{A}\} + (1-d) \cdot \{\text{C}_3\text{S}\}] + b \quad (14)$$

A linear relationship between cement characteristics and flow resistance was however not found to be a universal rule as illustrated by pastes with 0.53% lignosulphonate in Fig. 10 and pastes with 0.53% RN-15 and 6.97 vol.% SF in Fig. 11. The figures illustrate that the paste of CEM I 42.5 RR has a much higher flow resistance than the others, resulting in an exponential

Table 6
Flow resistance as a function of time, cement and plasticizer type

Plasticizer	Cement number	Flow resistance (Pa/s)			
		1st cycle	2nd cycle	3rd cycle	4th cycle
SNF	1	8593	9875	11,720	16,500
	2	1797	2084	2490	2922
	3	3096	3817	4548	5370
	4	250	249	260	282
	5	364	376	432	495
	6	936	1131	1373	1616
PA	1	1736	1819	2053	2436
	2	561	519	530	552
	3	738	595	581	576
	4	55	152	152	159
	5	61	122	132	139
LS	1	2460	2099	2092	2155
	2	529	361	382	382
	3	541	546	568	587
	4	278	205	208	237
	5	293	259	270	273

All cement pastes are prepared with w/c = 0.40 and 0.53% plasticizer by cement weight and the flow resistance data are taken from the medium shear rate range (152–118 s^{-1}).

correlation between flow resistance and cement characteristics similar to the correlation found for cement fineness and flow resistance in Fig. 2. The relationship between flow resistance and cement characteristics will in this case follow Eq. (15).

$$\text{Flow Resistance} = a \cdot \exp\left(b \cdot \text{Blaine} \cdot \{d \cdot \text{cC}_3\text{A} + (1-d) \cdot \text{C}_3\text{S}\}\right) \quad (15)$$

The reason for the exponential growth of flow resistance might be influenced by the various finenesses and also possibly the C_3A content of the different cements. Another possible explanation might be the different cement-plasticizer interactions. All cements have different saturation dosages of plasticizers as depicted for lignosulphonate and SNF in Table 5. The data illustrate that the saturation dosage depends on the cement type: A CEM I 42.5 RR paste has for example a plasticizer saturation dosage which is more than 3 times the saturation dosage for CEM I 52.5 R-LA cement.

Another consequence of plasticizer addition is retardation of the cement hydration. The extent of retardation depends on cement type, plasticizer type and dosage. Lignosulphonate has been found to be the strongest retarder while SNF is the weakest of the three plasticizers studied at high dosages. Pastes with plasticizer dosages below saturation will generally hydrate faster than supersaturated pastes. The particularly high flow resistance of CEM I 42.5 RR cement compared to the others might thus be caused by that this cement is under-plasticized at a plasticizer dosage of 0.53% SNF and lignosulphonate while some of the other cements are supersaturated. CEM I 42.5 RR has a relatively high surface area and C_3A content which cause a relatively high plasticizer saturation dosage and hydration rate compared to the other cements. The comparatively high hydration rate will in turn lead to a relatively high flow resistance due to consumption of water and precipitation of hydrate phases. The hydration of CEM I 42.5 RR will thus not be as retarded by the plasticizers as the others.

The flow resistance can increase or decrease with time during the initial hydration (dormant period): It will increase relative more with time for the cements with higher value of the cement characteristic Blaine·[d·{cubic C_3A}+(1−d)·{C_3S}] than for those with lower value, since higher specific surface and higher content of cubic C_3A lead to more surface hydration and thereby higher viscosity due to removal of water to form surface hydrates. Rate of flow loss depends also on the plasticizer type. It can be seen from Table 6 that pastes with lignosulphonate generally developed lower flow loss rates than pastes with SNF. Similar results have been found by Uchikawa et al. [9] who found that lignosulphonate formed complex salts with Ca^{2+} more easily than SNF. The lignosulphonate-Ca^{2+} complexation delays Ca^{2+} saturation in the pore water and thus the setting time. Table 6 shows further that pastes with polyacrylate roughly maintain the flow resistance values within the 4 measurement cycles. Similar results have been found by Golaszewski and Szwabowski [19] who found that the rate of change of the yield stress with time was clearly lower for mortars with polyacrylate plasticizer than for pastes with SNF. They found moreover that the values of viscosities generally decreased with time.

Tables 7 and 8 cite the measured effect of time (i.e. correlation at 25 min cycles) on the *linear* correlation variables a, b and d. Table 7 represent pastes with 0.53% by cement weight SNF which obtain flow loss (increased flow resistance) within the 2 h of rheological measurements. It can be seen from the data and in Fig. 12 that the values of b decrease while the values of a increase given that d is constant.

Table 7
Linear correlation parameters for the cement characteristics of cements 1–6 versus area under flow curve for medium shear rate range (upper value) and low shear rate range (lower value) when 0.53% naphthalene sulphonate-formaldehyde condensate (SNF) is used as plasticizer

Shear rate range	Parameter	1st cycle	2nd cycle	3rd cycle	4th cycle
Medium	R^2	0.9908	0.9928	0.9932	0.9842
Low		0.9973	0.9939	0.9905	0.9957
Medium	a	2.40	2.77	3.29	4.65
Low		1.69	1.84	2.05	2.57
Medium	b	−3967	−4547	−5417	−8019
Low		−2428	−2554	−2529	−3254
Medium	d	0.940	0.940	0.940	0.940
Low		0.945	0.95	0.955	0.955

Table 8
Linear correlation parameters for the cement characteristics of cements 1–6 versus area under flow curve for medium shear rate range (upper value) and low shear rate range (lower value) when 0.53% polyether grafted polyacrylate (PA) is used as plasticizer

Shear rate range	Parameter	1st cycle	2nd cycle	3rd cycle	4th cycle
Medium	R^2	0.9996	0.9793	0.9675	0.9521
Low		0.9794	0.9579	0.9454	0.9333
Medium	a	0.53	0.49	0.54	0.62
Low		0.23	0.29	0.30	0.34
Medium	b	−311	−629	−978	−1410
Low		−621	−673	−989	−1222
Medium	d	0.980	0.950	0.930	0.915
Low		0.935	0.900	0.880	0.870

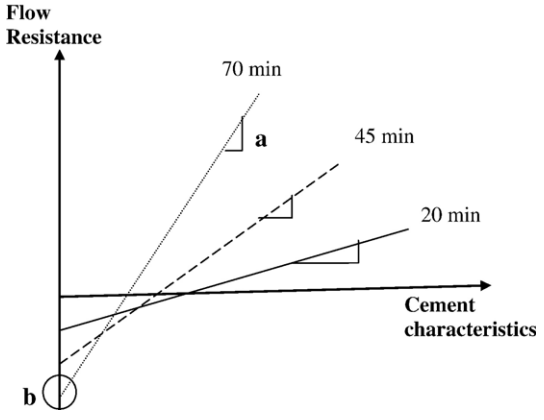

Fig. 12. Illustration of how the linear regression parameters a and b from Eq. (14), Flow Resistance=a·Blaine·{d·cC$_3$A+(1−d)·C$_3$S}+b, change with time provided that the relative reactivity factor, d, is constant.

Table 9
Exponential correlation parameters for the cement characteristics of cements 1–5 versus area under flow curve for medium shear rate range (upper value) and low shear rate range (lower value) when 0.53% lignosulphonate is used as plasticizer

Shear rate range	Parameter	1st cycle	2nd cycle	3rd cycle	4th cycle
Medium	R^2	0.9871	0.9997	0.9991	0.9979
Low		0.9912	0.9846	0.9641	0.9805
Medium	a	146.88	45.45	54.2	66.06
Low		0.4644	0.5035	0.4375	0.1527
Medium	b	$658 \cdot 10^{-6}$	$597 \cdot 10^{-6}$	$600 \cdot 10^{-6}$	$601 \cdot 10^{-6}$
Low		$919 \cdot 10^{-6}$	$962 \cdot 10^{-6}$	$974 \cdot 10^{-6}$	$865 \cdot 10^{-6}$
Medium	d	0.97	0.90	0.91	0.92
Low		0.83	0.85	0.85	0.78

The pastes in Table 8 represent pastes with 0.53% PA by cement weight which obtain both slight flow gain and flow loss. The data illustrate that the values of a increase slightly with time while the values of b decrease markedly. The relative reactivity fraction d is found to decrease with time which has a strong influence on the flow resistance values since the influence of C_3S content increase.

Table 8 illustrates furthermore that the linear regression parameter, R^2, decreases with time. This might be caused by the different hydration rates of the various cements. CEM I 42.5 RR cement hydrates particularly fast compared to the other cements due to its high surface and C_3A content. The decline in the regression parameter might also be caused by reduced reproducibility with time.

Table 9 depicts the measured effect of time on the *exponential* correlation variables a, b and d. The pastes represented in Table 9 were added 0.53% lignosulphonate and obtained slight flow loss following initial flow gain as seen from Table 6. It can be seen that the values of b are close to constant with time. The values of a and d decrease initially before they increase slightly from the 2nd to the 4th cycle.

It can be seen from Tables 8 and 9 that the values of the relative reactivity factor, d, have been found to be lower at the low shear rate (43–8.8 s^{-1}) range compared to the medium shear rate range (152–118 s^{-1}). This might imply that the influence of the hydration products of C_3S is stronger on the flow resistance at low shear rates compared to those of C_3A.

5. Conclusions

The polyacrylate was the most efficient plasticizer of the three tested while SNF and lignosulphonate gave comparable results. Lignosulphonate was furthermore found to have the strongest retarding effect on the setting times while SNF had the least influence on the setting times.

There is a correlation between the cement characteristic; Blaine$\cdot\{d\cdot cC_3A+(1-d)\cdot C_3S\}$ and the "flow resistance" measured as the area below the flow curve for selected shear rate ranges. The flow resistance is either a linear or exponential function of the cement characteristics depending on the plasticizer type and dosage (i.e. the retarding effect on the hydration).

The minerals must be determined by Rietveld analysis of XRD and holds then for a mix of pure cement and cement with fly ash, limestone filler (4%), as well as paste with constant silica fume dosage.

Acknowledgement

We would like to thank Dr. Thomas Füllmann for performing the Rietveld analysis of the cements used in this work at the Laboratory of Construction Materials, EPFL, Lausanne, Switzerland.

References

[1] M. Nehdi, M.-A. Rahman, Estimating rheological properties of cement pastes using various rheological models for different test geometry, gap and surface friction, Cem. Concr. Res. 34 (2004) 1993–2007.
[2] M. Collepardi, The rheological behaviour of cement pastes, Il Cemento 68 (1971) 99–106.
[3] A.M.M. Sheinn, D.W.S. HO, C.T. Tam, Rheological model for self-compacting concrete—paste rheology, in: C.T. Tam (Ed.), Proceedings of the 27th Conference on Our World in Concrete and Structures, Singapore, CI-Premier, Singapore, 28–29 August 2002, pp. 517–523.
[4] S. Greszczyk, L. Kucharska, The Influence of Chemical Composition of Cement on the Rheological Properties, From the Proceedings of the International Conference organized by The British Society of Rheology; "Rheology of Fresh Cement and Concrete" Edited by P.F.G Banfill, The British Society of Rheology, E.& F.F. Spon, London 1990.
[5] P.F.G. Banfill, A viscometric study of cement pastes containing superplasticizers with a note on experimental techniques, Mag. Concr. Res. 33 (1981) 37–47.
[6] J.A. Lewis, H. Matsuyama, G. Kirby, S. Morisette, J.F. Young, Polyelectrolyte effects on the rheological properties of concentrated cement suspensions, J. Am. Ceram. Soc. 83 (8) (2000) 1905–1913.
[7] I. Odler, T. Becker, Effect of some liquefying agents on properties and hydration of Portland cement and tricalcium silicate pastes, Cem. Concr. Res. 10 (3) (1980) 321–331.
[8] H. Uchikawa, S. Hanehara, T. Shirasaka, D. Sawaki, Effect of admixture on hydration of cement, adsorptive behavior of admixture and fluidity and setting of fresh cement paste, Cem. Concr. Res. 22 (6) (1992) 1115–1129.
[9] H. Uchikawa, S. Hanehara, D. Sawaki, The role of steric repulsive force in the dispersion of cement particles in fresh paste prepared with organic admixture, Cem. Concr. Res. 27 (1) (1997) 37–50.
[10] S. Chandra, J. Björnström, Influence of cement and superplasticizers type and dosage on the fluidity of cement mortars—Part I, Cem. Concr. Res. 32 (2002) 1605–1611.
[11] S. Chandra, J. Björnström, Influence of cement and superplasticizers type and dosage on the slump loss of Portland cement mortars—Part II, Cem. Concr. Res. 32 (2002) 1613–1619.
[12] R.M. Turian, T.W. Ma, F.L.G. Hsu, D.J. Sung, Characterization, settling, and rheology of concentrated fine particulate mineral slurries, Powder Technol. 93 (1997) 219–233.

[13] A. Yahia, K.H. Khayat, Analytical models for estimating yield stress of high-performance pseudoplastic grout, Cem. Concr. Res. 31 (2001) 731–738.
[14] C. Atzeni, C. Massida, U. Sanna, Comparison between rheological models for Portland cement pastes, Cem. Concr. Res. 15 (1985) 511–519.
[15] A. Yahia, K.H. Khayat, Applicability of rheological models to high-performance grouts containing supplementary cementitious materials and viscosity enhancing admixture, Mat. Struct. 36 (2003) 402–412.
[16] E.A.M. Gad, M.R. Mabrouk, F.H. Mosallamy, Rheological properties of different cement pastes made with different admixtures, Silic. Ind. 70 (3,4) (2005) 59–64.
[17] G. Walenta, T. Füllmann, Advances in quantitative XRD analysis for clinker, cements and cementitious additions, Powder Diffr. 19 (1) (2004) 40–44.
[18] K.L. Scrivener, T. Füllmann, E. Gallucci, G. Walenta, E. Bermejo, Quantitative study of Portland cement hydration by X-ray diffraction/Rietveld analysis and independent methods, Cem. Concr. Res. 34 (2004) 1447–1541.
[19] J. Golaszewski, J. Szwabowski, The Influence of superplasticizers on the rheological behaviour of fresh cement mortars, Cem. Concr. Res. 34 (2004) 235–248.
[20] S. Hanehara, K. Yamada, Interaction between cement and chemical admixture from the point of cement hydration, absorption behaviour of admixture, and paste rheology, Cem. Concr. Res. 29 (1999) 1159–1165.
[21] H. Vikan, "Rheology and reactivity of cementitious binders with plasticizers", Doctoral Theses at NTNU 2005:189, also available at http://www.diva-portal.org/ntnu/theses/abstract.xsql?dbid=689.
[22] A.I. Boikova, A.I. Domansky, V.A. Paramonova, G.P. Straviskaja, V.M. Nikuschenko, The influence of Na_2O on the structure and properties of $3CaO.Al_2O_3$, Cem. Concr. Res. 7 (1977) 483–492.
[23] N. Bilanda, P. Fierens, J. Tirlocq, N. Tenoutasse, Hydration of tricalcium aluminate doped by sodium oxide, 7th International Congress on the Chemistry of Cement, vol. IV, Editions Septima, Paris, 1980.